Impact of doping on the density of states and the mobility in organic semiconductors

Guangzheng Zuo, Hassan Abdalla, and Martijn Kemerink*
Complex Materials and Devices, Department of Physics, Chemistry and Biology, Linköping University, 58183 Linköping, Sweden
(Received 6 April 2016; published 27 June 2016)

We experimentally investigated conductivity and mobility of poly(3-hexylthiophene) (P3HT) doped with tetrafluorotetracyanoquinodimethane (F_4TCNQ) for various relative doping concentrations ranging from ultralow (10^{-5}) to high (10^{-1}) and various active layer thicknesses. Although the measured conductivity monotonously increases with increasing doping concentration, the mobilities decrease, in agreement with previously published work. Additionally, we developed a simple yet quantitative model to rationalize the results on basis of a modification of the density of states (DOS) by the Coulomb potentials of ionized dopants. The DOS was integrated in a three-dimensional (3D) hopping formalism in which parameters such as energetic disorder, intersite distance, energy level difference, and temperature were varied. We compared predictions of our model as well as those of a previously developed model to kinetic Monte Carlo (MC) modeling and found that only the former model accurately reproduces the mobility of MC modeling in a large part of the parameter space. Importantly, both our model and MC simulations are in good agreement with experiments; the crucial ingredient to both is the formation of a deep trap tail in the Gaussian DOS with increasing doping concentration.

DOI: 10.1103/PhysRevB.93.235203

I. INTRODUCTION

Molecular doping is an effective way to greatly increase the conductivity of organic semiconductors, which is more and more used in applications such as light emitting diodes, solar cells, and thermoelectric generators [1–5]. It has been found that a conductivity increase of four orders of magnitude or more can be achieved for various polymer/molecular dopant systems [6–8]. In a number of papers, a formal description of this behavior is presented, but convergence regarding the preferred formalism has not yet been reached [9–14]. A focus of research thus far has been to explain the nonmonotonic dependence of the carrier mobility on the dopant concentration, which is consistently observed in experiments. Poly(3-hexylthiophene) (P3HT) has been the key model system for investigating the effect of molecular doping. The evolution of the conductivity with increasing doping consistently exhibits a roughly log-linear behavior, with two distinct regimes characterized by a difference in inclination. Experimentally, it has been found that the hole mobility decreases with increasing doping level at low to moderate doping, before increasing steeply at higher doping levels, such that the conductivity increases sublinearly at first and superlinearly at higher doping levels. Both conductivity and mobility exhibit a maximum at around 20% dopant concentration, and a third regime may be defined beyond that level in which mobility and conductivity rapidly decrease [7,8]. Additionally, the magnitude of the mobility depends strongly on the regio-regularity of P3HT and has been found to increase over several orders of magnitude with crystallinity [15]. However, the nonmonotony of the mobility remains. In a first attempt to theoretically treat this effect of doping on the mobility in disordered organic semiconductors, Arkhipov *et al.* assumed that ions introduced by doping act as Coulombic traps that sit deep in the tail of the density of states (DOS) of the intrinsic system [11,12]. Upon adding dopant ions, shallow hopping sites are converted into deep sites, thereby broadening the tail of the DOS and decreasing the mobility. Simultaneously, the number of additional charge carriers increases with doping, which results in a sublinear increase of conductivity. At higher doping levels, the Coulomb potentials of the individual doping-induced traps start to overlap, thus smoothing out the energy landscape with every added dopant ion, thereby making it easier for a carrier to escape the trap. This circumstance in combination with the filling of the low-mobility tail states by the additional doping-induced free charges leads, in this model, to the increase of the conductivity at high doping ratios. This model aims to describe both the field and temperature dependence of the mobility as well as the nonmonotonous behavior of the mobility upon molecular doping and has been successfully fitted to experiments by Pingel *et al.* [16] and Pingel and Neher [17].

Intriguingly, Zhang and Blom [13] and Maennig *et al.* [9] could accurately describe the concentration, field, and temperature dependencies of the *p*-type conductivity in tetrafluorotetracyanoquinodimethane (F_4TCNQ)-doped organic semiconductors on the basis of models that do not account for modification of the DOS by the potential of the ionized dopants and that therefore predict a monotonous increase of the mobility with doping concentration due to state filling effects. These models were extended by Schmechel [10] and later Tietze *et al.* [18,19] by phenomenological inclusion of dopant-induced trap levels inside the bandgap. None of these models has been benchmarked against numerically exact kinetic Monte Carlo (MC) or similar calculations.

Here, we give a simple yet quantitative analysis of the impact of doping on the hole mobility in organic disordered semiconductors, based on a new model that assumes a doping-induced modification of the intrinsic Gaussian DOS. This model accurately reproduces the mobility of kinetic MC modeling in a large part of the parameter space, in contrast to the model by Arkhipov *et al.* [11,12]. In addition, the experimental mobility of P3HT doped by F_4TCNQ was investigated by varying the doping concentration from ultralow (10^{-5}) to high (10^{-1}); the results, showing a nonmonotonic

*martijn.kemerink@liu.se

 ©2016 American Physical Society

concentration dependence of the mobility, are found to be in good agreement with the new model and MC modeling. Finally, we found that the accurate measurement of the doping-induced Ohmic conductivity in diode-type devices requires a minimum film thickness that depends on concentration.

Above, and in the following, we follow literature convention to use the term doping for all guest (F_4TCNQ) concentrations, even though, strictly spoken, this is incorrect. At guest concentrations around and above 10^{-1}, transport between guest sites becomes relevant, and the system should rather be considered a blend with transport dominated by the merged DOS of both materials.

II. RESULTS AND DISCUSSION

A. Model description

In this paper, two simple analytical models for the conductivity σ and mobility μ are compared with brute force kinetic MC simulations. All simulations are based on a hopping formalism that takes the specific shape of the density of single particle states $g(E)$ as input along with physical parameters.

The hopping formalism is based on the Mott-Martens model as described by Coehoorn *et al.* [20] and that was previously used to calculate the transfer characteristics of field effect transistors [21,22]. In this model, the conductivity is calculated from a Miller-Abrahams-type expression

$$\sigma = \sigma_0 \exp\left(-2\alpha R^* - \frac{E^* - E_F}{k_B T}\right), \tag{1}$$

with σ_0 being a conductivity prefactor. The conductivity determining hops are assumed to take place over a distance R^* and to go from the Fermi energy E_F to an energy E^*. R^* and E^* are related through the DOS $g(E)$ as

$$B_C = \frac{4}{3}\pi (R^*)^3 \int_{E_F}^{E^*} g(E)dE, \tag{2}$$

where $B_C = 2.8$ is the critical number of bonds on the percolating network. For variable range hopping systems, the conductivity is obtained by maximizing Eq. (1) under the condition set by Eq. (2). As nearest-neighbor hopping models are found to give an excellent description of the charge transport in disordered organic semiconductors [20,23], we shall benchmark our models to a kinetic MC model based on nearest-neighbor hopping that will be described below. In this case, $R^* = a_{NN}$, it is more appropriate to drop Eq. (2) and assume hops take place to a fixed critical energy E_{crit}. For a purely Gaussian DOS of width σ_{DOS} and Millar Abrahams hopping on a cubic lattice, Cottaar *et al.* have shown that $E_{crit} = -0.491\sigma_{DOS}$ below the center of the DOS [24]. Here, we assume that this relation also holds for densities of states that are perturbed by the presence of ionic species, i.e., $E^* = E_{crit}$. For the asymmetric DOS derived below, E^* is calculated with respect to the DOS maximum.

Both analytical models are based on the idea that the original Gaussian DOS

$$g_i(E) = \frac{N_i}{\sqrt{2\pi}\sigma_{DOS}} \exp\left(-\frac{(E - E_i)^2}{2\sigma_{DOS}^2}\right), \tag{3}$$

with N_i being the total DOS and E_i being the central highest occupied molecular orbital (HOMO) or lowest unoccupied molecular orbital (LUMO) energy of the considered band, is extended towards low energies by the attractive Coulomb potential of ionized dopants.

The first analytical model (model I) follows the work of Arkhipov *et al.* in Ref. [12]. This model was recently used by Pingel and Neher to successfully interpret the concentration dependence of the conductivity of F_4TCNQ-doped poly 3-hexylthiophene (P3HT) [17]. For completeness, the key expressions will be given here. The randomly dispersed ionized dopants give rise to a correlated potential landscape of Coulomb traps separated by barriers of height Δ. It is assumed that (i) every Coulomb trap can be replaced by a single deep localized state nearest to the ionized dopant and (ii) the energy of this site is a sum of the intrinsic disorder energy and the barrier Δ [12]. The DOS then becomes

$$g(E) = \frac{N_i - N_d}{N_i} g_i(E) + \frac{N_d}{N_i} g_i\left(E + \frac{q^2}{4\pi\varepsilon_0 a} + U_m\right), \tag{4}$$

with N_d being the doping density. As a is the typical distance between the dopant ion and the trapped charge carrier, the second term between brackets can be associated with the binding energy, $E_{binding}$, between the dopant ion and the charge carrier. U_m is the maximum of the net potential formed by the overlapping Coulomb potentials of neighboring dopant ions in the presence of an externally applied electrostatic field [12]. Qualitatively, Eq. (4) describes the DOS of a doped organic semiconductor as a slightly reduced intrinsic DOS $g_i(E)$ plus a smaller, downward shifted copy of $g_i(E)$. The magnitude of this copy is proportional to the doping concentration; its downward shift gets smaller with increasing doping concentration and electric field. Hence, the doping-induced traps get more abundant but shallower with increasing doping concentration.

The second analytical model (model II) employs a DOS that was obtained by Arkhipov *et al.* by statistical evaluation of all possible separation distances between a charge and the nearest dopant ion [11]. Using the probability distribution to find the nearest doping ion at a distance r to weigh the Coulomb interaction, $E_C(r) = -q^2/4\pi\varepsilon_0\varepsilon_r r$ leads to the following energy distribution function in the doped material [11],

$$g(E) = A \int_{-\infty}^{0} \frac{dE_c}{E_C^4} \exp\left(\frac{A}{3E_C^3}\right) g_i(E - E_C), \tag{5}$$

with $A = \frac{4\pi q^6 N_d}{(4\pi\varepsilon_0\varepsilon_r)^3}$ and ε_r being the relative dielectric constant of the semiconductor, here taken as 3.6. In its original shape, Eq. (5) cannot account for energy level differences between the dopant and the semiconductor, $\Delta E = E_d - E_i$ with E_d being the relevant energy level of the dopant. Defining $E_1 = E_C(N_i^{-1/3})$ as the Coulomb energy, one lattice constant away from the ionized dopant we write for the DOS

$$g(E) = \frac{N_i - N_d}{N_i} A \int_{E_1}^{0} \frac{dE_c}{E_C^4} \exp\left(\frac{A}{3E_C^3}\right) g_i(E - E_C) + \frac{N_d}{N_i} A \int_{-\infty}^{E_1} \frac{dE_c}{E_C^4} \exp\left(\frac{A}{3E_C^3}\right) g_i(E - \Delta E - E_C). \tag{6}$$

Qualitatively, Eq. (6) implies that within a radius $a_{\mathrm{NN}} = N_i^{-1/3}$ from the dopant, the original semiconductor is replaced by an (effective) dopant, consisting of an energy level at E_d and an ion. For simplicity, the disorder in the dopant site energies is assumed to be equal to that of the semiconductor. The on-site Coulomb binding energy $E_C(0)$ will in actual devices be of the order of $-0.5\ldots-1$ eV, which is easily implemented by setting the lower limit of the integral in the second term in Eq. (6) to $E_C(0)$.

The kinetic MC model has been extensively described before [25,26]. In brief, it accounts for nearest-neighbor hopping with Miller-Abrahams rates, c.f. Eq. (1), on a simple cubic lattice with lattice constant a_{NN}. Site energies are randomly drawn from a purely Gaussian DOS and corrected for external fields and the Coulomb interactions with all charged (electronic and ionic) particles. Coulomb interactions are exactly accounted for and updated upon every move of an electronic charge. The modification of the Gaussian DOS by the ionic charges is therefore exactly accounted for instead of through the approximations [Eq. (4) or (6)]. The on-site charge-ion Coulomb interaction $E_C(0)$ is truncated at -0.5 eV in analogy with the exciton binding energy.

For quantitative comparison with the kinetic MC model, the conductivity prefactor σ_0 in Eq. (1) is calculated from the Einstein relation as

$$\sigma_0 = n\mu_0 = n\frac{a_{\mathrm{NN}}^2\nu_0}{6k_BT}, \tag{7}$$

with ν_0 as the attempt-to-hop frequency and n as the charge carrier density that is set equal to the doping concentration N_d-, i.e., full integer charge transfer (CT) is assumed [8,17,27]. For both the analytical models and MC, mobilities are calculated from conductivities by dividing by the dopant concentration, giving the mean mobility for all available charges.

In the standard parameter set that is used unless indicated otherwise, the attempt to hop frequency $\nu_0 = 1e\text{-}11\,\mathrm{s}^{-1}$; intersite distance $a_{\mathrm{NN}} = 1.8$ nm; Gaussian disorder $\sigma_{\mathrm{DOS}} = 0.075$ eV; temperature $T = 300$ K; energy level difference $\Delta E = 0$; $E_{\mathrm{binding}} = -E_C(0) = 0.5$ eV.

B. Hole mobility

In Fig. 1, the hole mobility calculated from model I for various values of the energetic disorder σ_{DOS} is compared to the results of the MC simulation. While the aforementioned nonmonotony of the mobility over the relevant doping range is present in both cases, model I deviates significantly from the exact MC simulation. Also, when varying other parameters like the HOMO-LUMO difference (ΔE) and the intersite distance (a_{NN}), it was found that the mobility calculated from model I was inconsistent with MC modeling, as shown in Figs. S1 and S2 in the Supplemental Material [28]. The reason that this model fails will be discussed in a later section.

It is important to note that the failure of model I is not due to the hopping model [Eqs. (1)–(3)]. To this end, we calculated mobilities vs free charge concentration for a wide range of parameters from both Eq. (1) and MC. By free, we mean charges that are not accompanied by an ion, so the intrinsic DOS [Eq. (3)] is used. The results in Figs. S4–S7 in the Supplemental Material [28] show almost exact correspondence between the two.

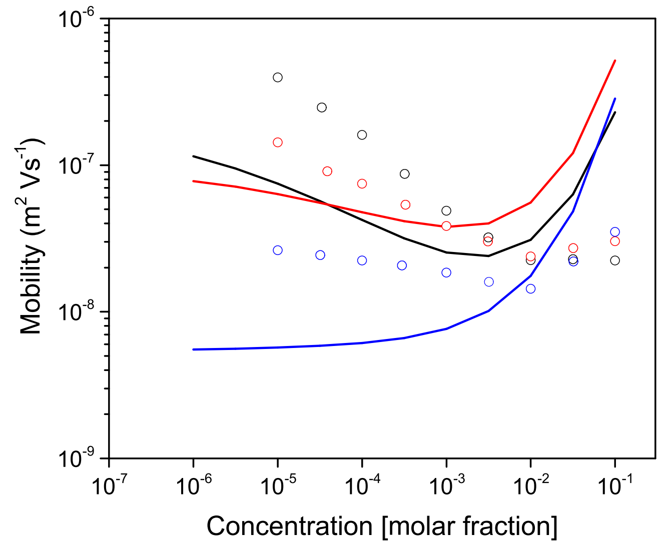

FIG. 1. Hole mobility from model I (solid lines) and MC (dots) using the standard parameter set. Energetic disorder is $\sigma_{\mathrm{DOS}} = 0.05$ eV (black), 0.075 eV (red), and 0.1 eV (blue).

We noticed that it is possible to reproduce the mobilities generated by MC by freely varying the parameters in model I, as shown in Fig. S3 (Supplemental Material [28]) but that the parameters extracted from this procedure deviate significantly from those used as input in the MC calculations. Model I may therefore give erroneous and/or misleading results when applied to real experiments.

In Fig. 2, the hole mobility calculated from model II and the MC simulation are plotted against doping concentration and parametric in energetic disorder, HOMO-LUMO difference, intersite distance, and temperature. The MC data set shown in Fig. 2 is the same as in Fig. 1. We consistently found that model II quite accurately reproduces the mobility of the MC modeling in a large part of the parameter space.

Figure 2(a) shows the hole mobility dependence on doping concentration for different values of the intrinsic energetic disorder. It is well known that the mobility decreases as disorder increases [20,23]. However, at high doping concentration the width of the DOS, and thereby the disorder, is dominated by the aforementioned broadening due to dopant ions, and the dependence of the mobility on intrinsic disorder can be expected to become reduced or to even vanish entirely. As can be seen in Fig. 2(a), this effect is quite well reproduced in both model II and the MC simulation. Also, the previously described nonmonotony of the mobility is well reproduced in Fig. 2(a), where the hole mobility decreases between a doping ratio of 10^{-6} to 10^{-2}, before increasing at around 10^{-1} for both model II and the MC modeling. It is noteworthy that while the mobility decreases by almost two orders of magnitude for the smallest disorder, it only decreases by about a factor of 2 for the largest disorder. This behavior can be explained by the fact that in the low to medium doping regime where dopant ions broaden the DOS towards the tail of the intrinsic DOS, the broadening due to doping is less relevant for an intrinsic DOS that is already relatively broad.

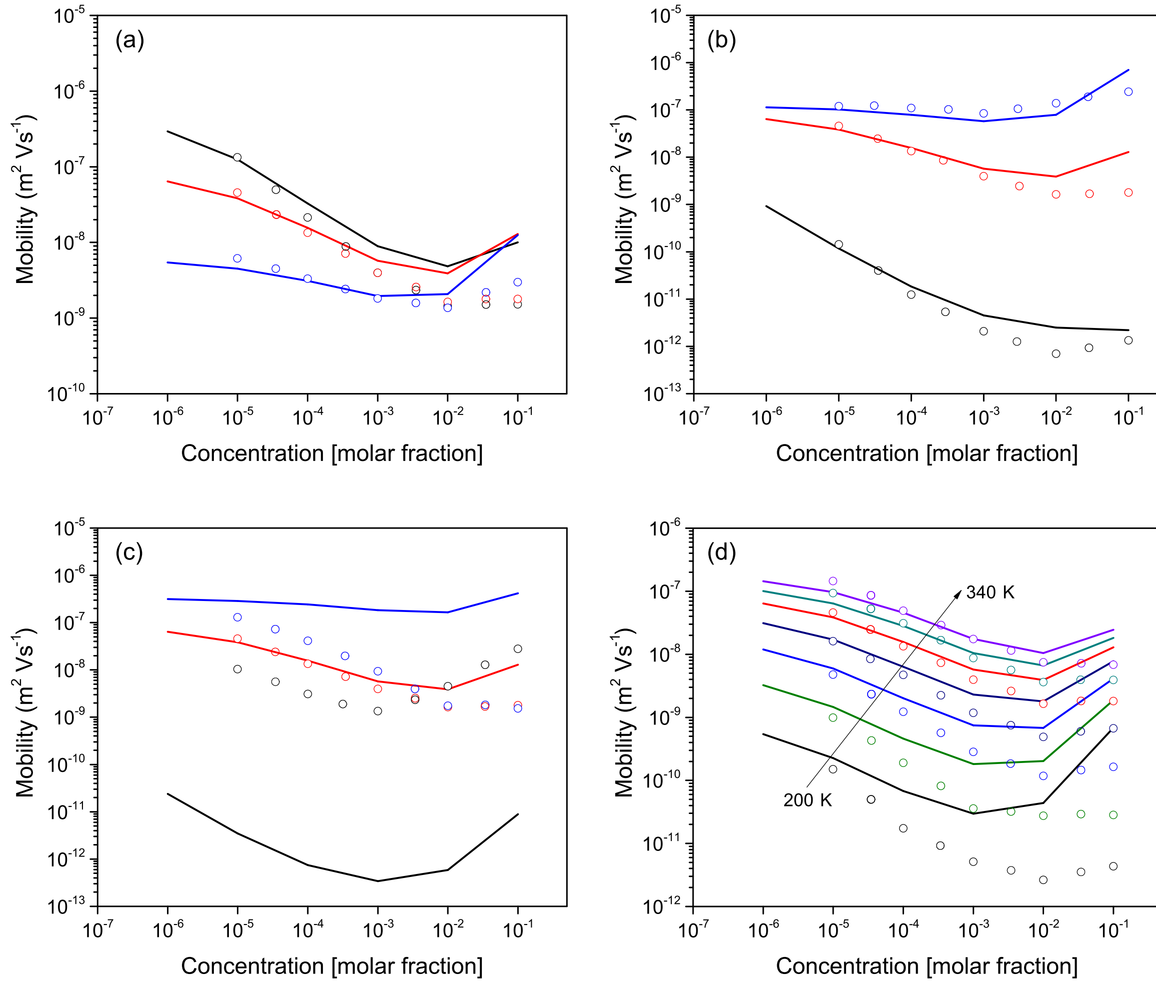

FIG. 2. Dependence of hole mobility on doping concentration from model II (solid lines) and MC (dots) for different parameters: (a) energetic disorder: $\sigma_{\mathrm{DOS}} = 0.05$ eV (black), 0.075 eV (red), and 0.1 eV (blue); (b) energy level difference: $\Delta E = -0.2$ eV (black), 0 eV (red), and 0.3 eV (blue); (c) intersite distance $a_{\mathrm{NN}} = 1.0$ nm (black), 1.8 nm (red), and 3.0 nm (blue); (d) temperature: $T = 200$ K, 225 K, 250 K, 275 K, 300 K, 320 K, and 340 K.

Figure 2(b) shows the doping dependence of the hole mobility for various energy level differences ΔE between the HOMO of the host material and the LUMO of the dopant material. Here, $\Delta E > 0$ means that the host material's HOMO is above the dopant's LUMO, which allows electrons to easily transfer to the dopant, thereby increasing the hole density in the host material and enhancing mobility. In the opposite case, when the host material's HOMO is below the dopant's LUMO ($\Delta E < 0$), it becomes harder for electrons to transfer to the dopant. Therefore, the hole mobility at $\Delta E = 0.3$ eV is highest among the three situations. The nonmonotonous relationship between mobility and doping concentration is observed regardless of the energy difference. Irrespective of ΔE, model II accurately reproduces the MC modeling.

The hole mobility dependence on doping concentration for different intersite distances is shown in Fig. 2(c). Clearly there are large discrepancies between model II and MC simulations, with the notable exception of the line corresponding to an intersite distance of 1.8 nm. We believe this to be due to the correlations between the site energies due to the long-range nature of the Coulomb potential that are ignored in Eqs. (5) and (6), as pointed out by Arkhipov [11]. Especially at shorter intersite distances, when the Coulomb energy is large compared to the other energy scales in the system, it may be expected that ignoring these correlations leads to a significant overestimation of the effect of the ionic potentials and thus to an underestimation of the mobility. For comparison, for intersite distances $a_{\mathrm{NN}} = 1.0$ nm, 1.8 nm, and 3.0 nm, one has $E_1 \approx 0.40$ eV, 0.22 eV, and 0.13 eV, respectively. Luckily, in previous papers, we found that an intersite distance $a_{\mathrm{NN}} = 1.8$ nm gives an accurate description of many phenomena in organic semiconductor devices [25,26].

In organic semiconductors, temperature is known to have a considerable influence on the mobility, and its effect for the present case is shown in Fig. 2(d). As expected, increasing the temperature results in an increase of the hole mobility between 200 K to 340 K. Inspecting the deviations between the model II outcomes and MC simulations at the lowest temperatures, we notice a striking similarity with the deviation at longer intersite distance in Fig. 2(c) (blue line and symbols). This might point at a similar underlying cause, correlation effects being neglected in the present simplified model. Speculating, the results in Figs. 2(c) and 2(d) hint at a criterion of the shape $E_1/(\sigma^2/k_B T) \approx 1$ for cancelation of errors related to

ignoring correlation effects. For comparison, at $T = 300$ and 200 K, one has $\sigma^2/k_BT \approx 0.22$ eV and 0.33 eV, respectively. A further analysis of correlation effects is postponed for a future work.

Summarizing the observations in Fig. 2, we see that our simple model II provides a rather accurate description of the numerically exact MC calculations in a significant and relevant part of the parameter space. In particular, the nonmonotonic dependence of mobility on doping concentration is a robust observation.

C. Charge carrier positions

Before turning to the charge distribution in energy space, it is interesting to briefly inspect the spatial distribution of the charge carriers with respect to the doping ions. In Fig. 3, we plotted the fraction of charges that sit at the position of a dopant ion; that sit one site away from a dopant, which we will refer to as the CT position [29]; and that are free, i.e., sitting elsewhere. Beyond a concentration $\sim 10^{-2}$, the free fraction decreases steeply for the simple statistical reason that there are hardly any sites left in the system that are not a dopant or a CT site. However, also at lower concentrations, the fraction of free charges decreases with increasing dopant concentration. This trend seems opposite to one of the key assumptions in model I, namely that the increased overlap between the Coulomb potentials of neighboring dopants smoothes out the total potential, facilitating escape from the Coulomb traps and thereby increasing the mobility. We suspect, however, that this effect is still operational but counteracted by the fact that with increasing concentration the time between escape from one Coulomb trap and capture by another also decreases: Although the time spent at an individual dopant site during a specific event goes down with doping concentration, the total time spent at dopant sites in general goes up.

Even though our simulations assume that all dopants produce a charge carrier, one can loosely define a doping efficiency from the data in Fig. 3, e.g., as the fraction of free charges or the fraction not sitting at a dopant site. Irrespective of the precise definition, this doping efficiency is substantially below unity in a large fraction of the parameter space.

D. Density of states

In order to further understand the differences between analytical models I and II, we compare the corresponding

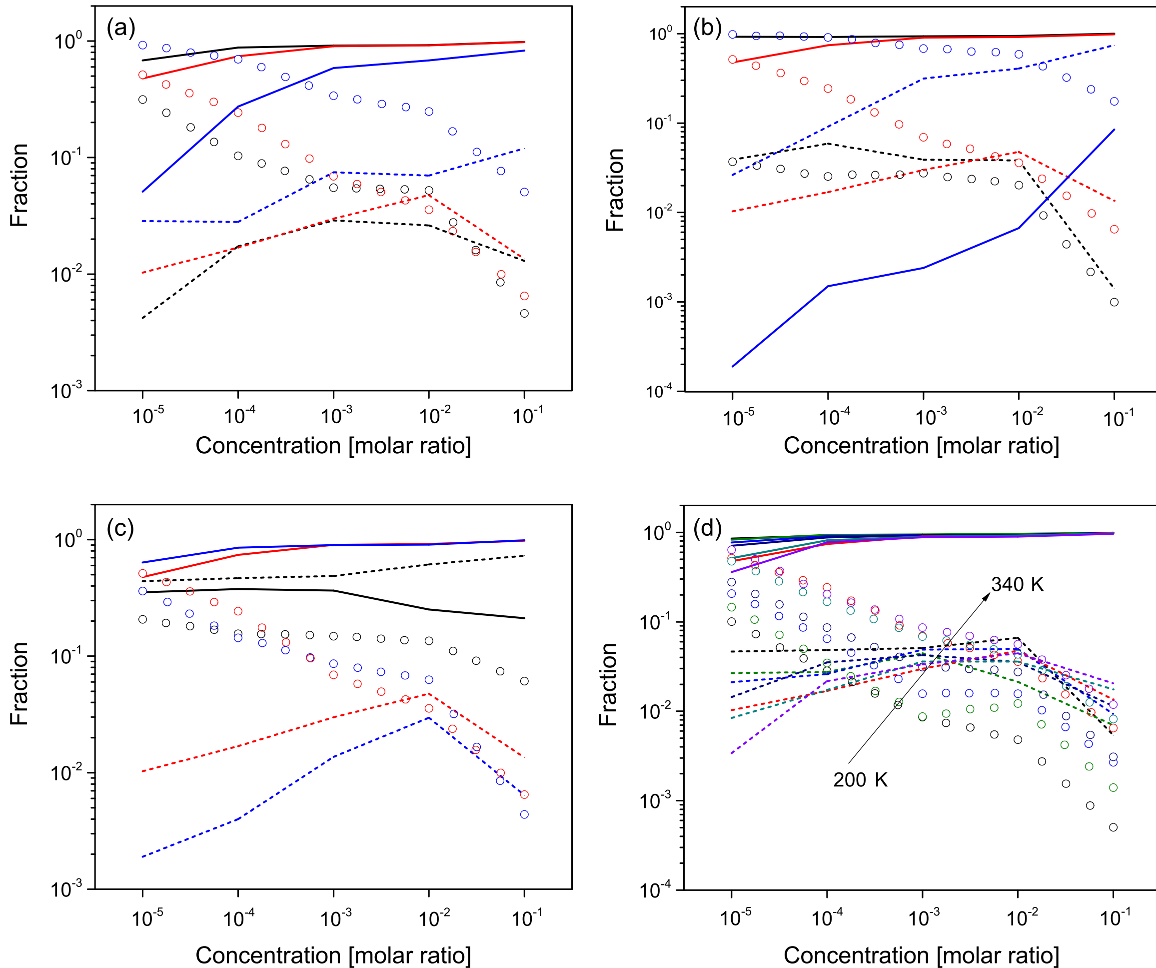

FIG. 3. Fraction of carrier charges at various positions: at dopant ions (solid lines), at CT position (dashed lines) and free (dots) vs doping concentration from MC for the same parameters as Fig. 2. (a) Energetic disorder: $\sigma_{\mathrm{DOS}} = 0.05$ eV (black), 0.075 eV (red), and 0.1 eV (blue); (b) energy level difference: $\Delta E = -0.2$ eV (black), 0 eV (red), and 0.3 eV (blue); (c) intersite distance: $a_{\mathrm{NN}} = 1.0$ nm (black), 1.8 nm (red), and 3.0 nm (blue); (d) temperature: $T = 200$ K, 225 K, 250 K, 275 K, 300 K, 320 K, and 340 K.

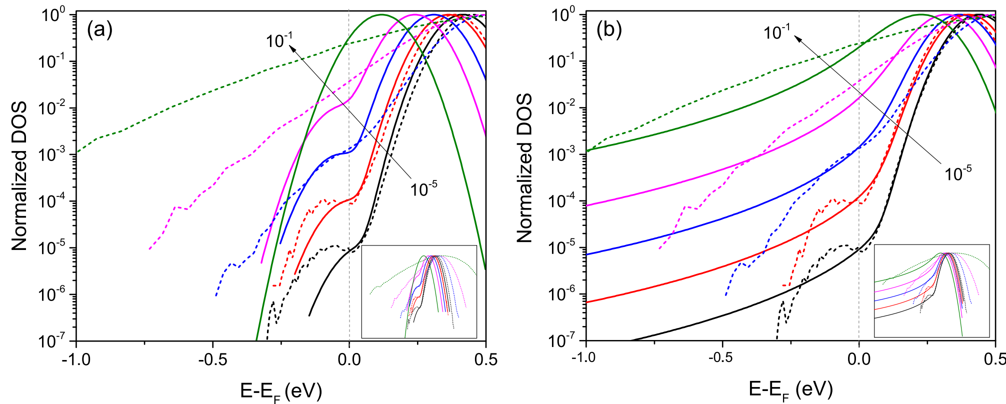

FIG. 4. DOS for different doping concentrations from (a) model I [Eq. (4), solid lines]; (b) model II [Eq. (6), solid lines], and MC (dashed lines) with the standard parameter set. The insets show the full energy scale.

approximate densities of states with the numerically exact DOS that is extracted from the MC simulation by a simple counting and binning procedure. The results are plotted in Fig. 4. Fermi levels are calculated separately in the three different models.

The key assumption in model I is that the Coulomb potential of each ion gives rise to a single trap site that shifts the original site energy by a certain amount that is equal for all dopants (but depends on concentration and field). Hence, they form a second Gaussian trap DOS distribution and do not affect the main intrinsic peak in the DOS distribution apart from a trivial downscaling. Neither the width of the intrinsic DOS nor the width of the trap DOS is assumed to depend on doping concentration. This is at odds with the actual DOS, as obtained from MC. As the critical hop in our transport model takes place between the Fermi energy and a state that sits roughly $\sigma_{\mathrm{DOS}}/2$ below the center of the main peak, the shape of the low-energy half of the main DOS peak is critical; deviations below E_F only matter when they lead to an erroneous position of E_F. Hence, on the basis of the deviating shape of the DOS, as predicted by Eq. (3), it may be expected that only at the lowest concentration (10^{-5}) the mobility prediction of model I will be accurate; at higher concentrations, the underestimation of the actual DOS width will lead to an overestimation of the mobility. The red line in Fig. 1 shows that this indeed is the case.

In model II, the ionic Coulomb potentials have the double effect on the DOS of adding a deep tail and to broadening the main peak. Both effects can also be seen in the MC simulations in Fig. 4(b); only for concentrations above $\sim 10^{-3}$ do deviations between the two become appreciable, in qualitative agreement with the trends in the mobility, c.f. the red lines and symbols in Fig. 2. The agreement and deviations in DOS shape at lower and higher concentrations, respectively, rationalize the consistent agreement and deviations between model II and the MC simulations at these limits. The roughly exponential shape of the dopant-induced tail states is likely the reason for the apparent success of mobility models that phenomenologically include an exponential or broad Gaussian tail of dopant-induced states [10,18,19]. Finally, we note that the strongest increase in effective width of the DOS occurs at the highest doping concentrations, in line with the results reported by Mityashin *et al.* on basis of a more detailed atomistic model [14].

E. Experiments

Hole-only devices were fabricated based on F_4TCNQ (LUMO: −5.24 eV) [30] doped P3HT (HOMO: −5.0 eV) [31]. To not obscure subtle yet important deviations from a strictly linear increase of the conductivity with doping concentration, we divided the measured Ohmic conductivity by the nominal doping concentration, giving an observable with the dimension of a mobility. Importantly, this mobility is directly comparable with the one from the simulations discussed above. In the case of integer CT with (nearly) unity efficiency, as has been observed for the P3HT:F_4TCNQ system [8,17,27], this is the actual mobility averaged over all charge carriers.

In order to avoid thickness-affected conductivities, we have investigated devices with various thickness of active layers. In

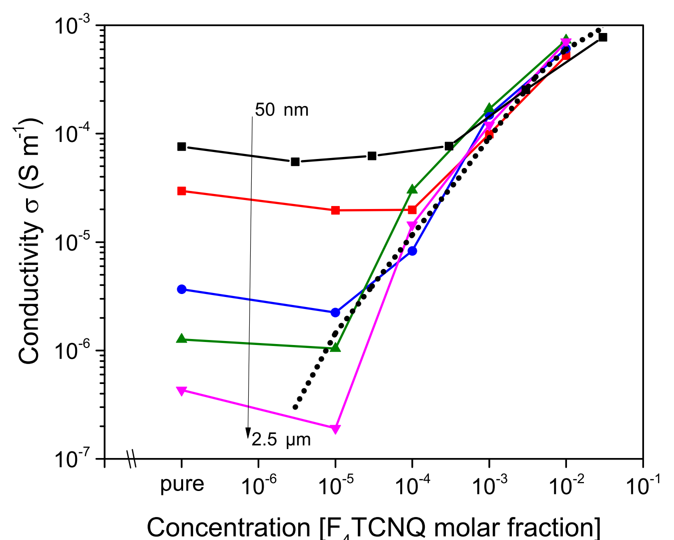

FIG. 5. Hole conductivity of P3HT vs F_4TCNQ concentration for different film thicknesses (symbols, solid lines connect the data points, thicknesses: 50 nm, 150 nm, 265 nm, 360 nm, and 2.5 μm). The dotted line is a manual spline through the data.

Fig. 5, the conductivity measured for P3HT is plotted against F_4TCNQ dopant concentration for various film thicknesses. Remarkably, the conductivity is especially sensitive to thickness in the ultralow doping range around 10^{-5}, the conductivity of thin films (50 nm) being more than two orders of magnitude higher than that of thick films (2.5 μm). It has previously been shown that diffusion of carriers from Ohmic contacts into the material creates a zone of increased conductivity close to the contacts [32]. For very thin films, this zone of extrinsic carriers fills a significant portion of the film leading to a greatly increased conductivity, as seen in Fig. 5. As a consequence, the conductivity remains relatively independent of doping concentration until the density of doping-induced charge carriers has surpassed the thickness dependent density of carriers injected from the contacts, at which point a steep, and thickness independent, increase is observed. Finally, the fact that the conductivity of undoped P3HT is a little bit higher than that of the low doped films is attributed to the Coulomb trap formation by dopant ions, which is extensively discussed above.

We have used the trend line in Fig. 5 to calculate the thickness-independent hole mobilities shown in Fig. 6. The mobility calculated from model II (lines) with $\Delta E =$ 0.2-0.3 eV shows excellent agreement with the experimental data in the low doping regime from 10^{-5} to $\sim 10^{-3}$ where, as anticipated, the mobility slowly decreases with doping concentration. It should be stressed that no fitting was done to match the shape of the model curves to the experiment—only the attempt to hop frequency ν_0 was set to the reasonable value of $5 \times 10^9\ s^{-1}$ to scale the absolute values. Otherwise, the model parameters have been chosen according to values commonly reported in literature for this type of system.

At high doping concentrations, the experimentally observed hole mobility decreases more strongly with an increasing amount of dopant. We believe this to be due to aggregation

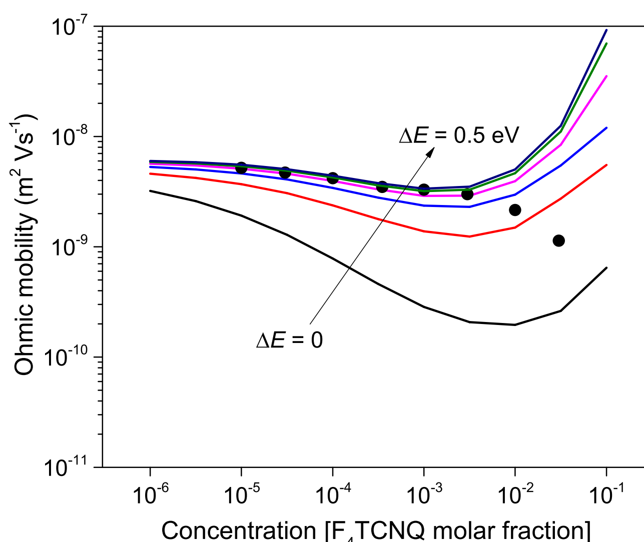

FIG. 6. Ohmic mobility dependence on F_4TCNQ concentration from experiments (black dots) and calculated from model II (solid lines) with different energy level differences ($\Delta E = 0$, 0.1, 0.2, 0.3, 0.4, and 0.5 eV). For P3HT:F_4TCNQ $\Delta E \approx 0.24$ eV.

of F_4TCNQ, setting in at concentrations around 10^{-2} [7]. In this context, dopant aggregation may be expected to have two effects on charge transport. First, it may destroy the crystalline morphology of the P3HT film, which can decrease the mobility. Secondl, it reduces the effective number of dopants, assuming an F_4TCNQ complex can only be singly ionized.

III. CONCLUSIONS

The hole mobility of *p*-type doped organic disordered semiconductors has been systematically analyzed by means of two analytical models, differing in the effect that the introduction of doping has on the intrinsic DOS distribution. While model I assumes that dopants create a second Gaussian DOS separate from the intrinsic DOS, model II assumes that doping causes a gradual broadening and the development of tail states. We compared both models to kinetic MC modeling of the same material as well as to measurements of F_4TCNQ-doped P3HT films. We find that model II accurately reproduces the doping dependence of mobility from MC modeling in a large part of the parameter space, while model I fails to do so. Furthermore, model II and MC modeling are in good agreement with experimental data, with some deviation in the high doping regime due to F_4TCNQ aggregation. In our diode-type devices, the conductivity is very sensitive to the thickness of the active layer, especially at ultralow doping regime, owing to additional charges diffusing in from Ohmic contacts.

ACKNOWLEDGMENTS

The research by G.Z. is supported by the Chinese Scholarship Council (CSC). We are grateful to Olle Inganäs for the use of technical infrastructure and to Nikolaos Felekidis, Olof Andersson, and Wanzhu Cai for useful discussions.

APPENDIX: EXPERIMENTS AND METHODS

1. Materials

Poly(3-hexylthiophene-2,5-diyl) (rr−P3HT, Mr = 166.3/repeat unit) and 2,3,5,6-Tetrafluoro-7,7,8,8-tetracyanoquinodimethane(F_4TCNQ, Mr = 276.15/repeatunit) were purchased from Sigma-Aldrich. F_4TCNQ was dissolved in o-DCB to make different solutions with concentrations from $1\ mg\ ml^{-1}$ to $10^{-4}\ mg\ ml^{-1}$. P3HT was dissolved in chloroform (CF) and added to the solution of F_4TCNQ to get a doping range from 10^{-5} to 10^{-1} (molar ratio). At the same time, we changed the concentration of P3HT in CF and the spin-coat speed used for the deposition of the active layer to get different thicknesses.

2. Device fabrication and measurement

Hole-only devices were fabricated with following structure: ITO/PEDOT:PSS (4083, 40 nm)/P3HT : F_4TCNQ/Mo_2O_3 (5 nm)/Al (90 nm). The active layers were spin-coated on the top of PEDOT:PSS film, and the thickness was 50 nm to 2.5 μm, as measured with a Dektak surface

profilometer. After that, the Al-contact was evaporated under the pressure of 1×10^{-6} mbar. The current-density vs voltage curves of all devices were measured in ambient air with a Keithley 2400.

Kinetic MC calculations were performed at doping concentrations of 10^{-5}, 10^{-4}, 10^{-3}, 10^{-2}, and 10^{-1} on boxes containing $(100\times100\times100)$, $(50\times50\times40)$, $(20\times20\times25)$, $(10\times10\times10)$, and $(10\times10\times10)$ sites, respectively. Other data points where generated by linear interpolation. For each concentration, results where averaged over at least 10 random configurations. Typically 10^7 hopping events where considered in each configuration to assure steady state had been reached.

[1] X. Zhou, J. Blochwitz, M. Pfeiffer, A. Nollau, T. Fritz, and K. Leo, Adv. Funct. Mater. **11**, 310 (2001).

[2] A. Loiudice, A. Rizzo, M. Biasiucci, and G. Gigli, J. Phys. Chem. Lett. **3**, 1908 (2012).

[3] K.-H. Yim, G. L. Whiting, C. E. Murphy, J. J. M. Halls, J. H. Burroughes, R. H. Friend, and J.-S. Kim, Adv. Mater. **20**, 3319 (2008).

[4] A. M. Glaudell, J. E. Cochran, S. N. Patel, and M. L. Chabinyc, Adv. Energy Mater. **5**, 1401072 (2015).

[5] Y. Zhang, H. Zhou, J. Seifter, L. Ying, A. Mikhailovsky, A. J. Heeger, G. C. Bazan, and T.-Q. Nguyen, Adv. Mater. **25**, 7038 (2013).

[6] P. Wei, J. H. Oh, G. Dong, and Z. Bao, J. Am. Chem. Soc. **132**, 8852 (2010).

[7] D. T. Duong, C. Wang, E. Antono, M. F. Toney, and A. Salleo, Org. Electron. **14**, 1330 (2013).

[8] I. Salzmann, G. Heimel, M. Oehzelt, S. Winkler, and N. Koch, Acc. Chem. Res. **49**, 370 (2016).

[9] B. Maennig, M. Pfeiffer, A. Nollau, X. Zhou, K. Leo, and P. Simon, Phys. Rev. B **64**, 195208 (2001).

[10] R. Schmechel, J. Appl. Phys. **93**, 4653 (2003).

[11] V. I. Arkhipov, P. Heremans, E. V. Emelianova, and H. Bässler, Phys. Rev. B **71**, 045214 (2005).

[12] V. I. Arkhipov, E. V. Emelianova, P. Heremans, and H. Bässler, Phys. Rev. B **72**, 235202 (2005).

[13] Y. Zhang and P. W. M. Blom, Org. Electron. **11**, 1261 (2010).

[14] A. Mityashin, Y. Olivier, T. Van Regemorter, C. Rolin, S. Verlaak, N. G. Martinelli, D. Beljonne, J. Cornil, J. Genoe, and P. Heremans, Adv. Mater. **24**, 1535 (2012).

[15] X. Jiang, Y. Harima, K. Yamashita, Y. Tada, J. Ohshita, and A. Kunai, Chem. Phys. Lett. **364**, 616 (2002).

[16] P. Pingel, R. Schwarzl, and D. Neher, Appl. Phys. Lett. **100**, 143303 (2012).

[17] P. Pingel and D. Neher, Phys. Rev. B **87**, 115209 (2013).

[18] M. L. Tietze, L. Burtone, M. Riede, B. Lüssem, and K. Leo, Phys. Rev. B **86**, 035320 (2012).

[19] M. L. Tietze, P. Pahner, K. Schmidt, K. Leo, and B. Lüssem, Adv. Funct. Mater. **25**, 2701 (2015).

[20] R. Coehoorn, W. F. Pasveer, P. A. Bobbert, and M. A. J. Michels, Phys. Rev. B **72**, 155206 (2005).

[21] W. S. C. Roelofs, S. G. J. Mathijssen, R. A. J. Janssen, D. M. de Leeuw, and M. Kemerink, Phys. Rev. B **85**, 085202 (2012).

[22] W. C. Germs, K. Guo, R. A. J. Janssen, and M. Kemerink, Phys. Rev. Lett. **109**, 016601 (2012).

[23] W. F. Pasveer, J. Cottaar, C. Tanase, R. Coehoorn, P. A. Bobbert, P. W. M. Blom, D. M. de Leeuw, and M. A. J. Michels, Phys. Rev. Lett. **94**, 206601 (2005).

[24] J. Cottaar, L. J. A. Koster, R. Coehoorn, and P. A. Bobbert, Phys. Rev. Lett. **107**, 136601 (2011).

[25] A. Melianas, V. Pranculis, A. Devižis, V. Gulbinas, O. Inganäs, and M. Kemerink, Adv. Funct. Mater. **24**, 4507 (2014).

[26] A. Melianas, F. Etzold, T. J. Savenije, F. Laquai, O. Inganäs, and M. Kemerink, Nat. Commun. **6**, 8778 (2015).

[27] C. Wang, D. T. Duong, K. Vandewal, J. Rivnay, and A. Salleo, Phys. Rev. B **91**, 085205 (2015).

[28] See Supplemental Material at http://link.aps.org/supplemental/10.1103/PhysRevB.93.235203 for a further analysis of model I and for plots of mobility vs free charge concentration.

[29] A. Y. Sosorev and D. Y. Paraschuk, Isr. J. Chem. **54**, 650 (2014).

[30] W. Gao and A. Kahn, Appl. Phys. Lett. **79**, 4040 (2001).

[31] M. D. Irwin, D. B. Buchholz, A. W. Hains, R. P. H. Chang, and T. J. Marks, Proc. Natl. Acad. Sci. USA **105**, 2783 (2008).

[32] N. I. Craciun, J. J. Brondijk, and P. W. M. Blom, Phys. Rev. B **77**, 035206 (2008).